Photoaligned Tunable Liquid Crystal Lenses with Parabolic Phase Profile

Svitlana Bielykh , Liana Lucchetti * , Victor Yu. Reshetnyak

Posted Date: 27 June 2023

doi: 10.20944/preprints202306.1931.v1

Keywords: liquid crystal lenses; modulated anchoring energy; spherical aberration; tunable focal length

Article

Photoaligned Tunable Liquid Crystal Lenses with Parabolic Phase Profile

S.P. Bielykh [1], L. Lucchetti [2,*], V. Yu. and Reshetnyak [1,3]

[1] Theoretical Physics Department, Physics Faculty, National Taras Shevchenko University of Kyiv, Volodymyrs'ka street 64, Kyiv, 01601, Ukraine
[2] Dipartimento SIMAU, Universita` Politecnica delle Marche, via Brecce Bianche, 60131 Ancona, Italy
[3] Department of Physics, University of Warwick, Coventry, CV4 7AL, UK
* Correspondence: l.lucchetti@univpm.it

Abstract: We present a theoretical modeling of a cylindrical tunable liquid crystal lens based on the modulation of the anchoring energy. This latter can be easily obtained by means of photoaligning techniques. The liquid crystal cell we propose exhibits strong anchoring at the top substrate and an anchoring energy with parabolic profile at the bottom substrate. The model describes the dependence of the focal length on the applied voltage and presents a theoretical study of lens aberrations. The results obtained are of general relevance and can be used to optimize the performances of every kind of liquid crystal lens with parabolic profile.

Keywords: liquid crystal lenses; modulated anchoring energy; spherical aberration; tunable focal length

Conventional lenses are based on the radial shaping of materials like glass or plastic that exhibits a constant refractive index. These optical components have typically one fixed focal length. The standard way of varying the focal length of an imaging system is thus to use a certain number of lenses such that the focus position is changed by mechanically adjusting their mutual distance. This approach makes the system bulky and unsuited for some applications. Compact and lightweight optical systems where the focal length can be varied without moving parts, are clearly very attractive. The fluid nature of the director field in liquid crystals (LC), combined with their high sensitivity to external stimuli, makes lenses based on liquid crystalline materials able to fulfill the above requirements. The focal length of LC lenses is typically electrically tunable and since the first report dated back to 1979 [1], several different structures have been proposed mainly based on patterned electrodes [2-7]. LC cells with pixel-free electrodes, have also been proposed [8].

Despite they are more than 40 years old and the large amount of existing literature, LC lenses continue to attract the interest of the scientific community due to the great number of possible applications. Some new devices, such as head-mounted displays, mobile cameras, or contact lenses have indeed demonstrated the need for novel adaptive lenses [9] and non-conventional solutions have been recently proposed [10-13].

With the aim of giving a contribution to the recent efforts, we propose here a theoretical study of LC lenses based on a parabolic profile of the anchoring energy that can easily be produced by photoalignment of proper transparent surface coatings [14-17]. Our simulations show that the application of an external voltage V in the range (0.7 – 1) V produces a tunable parabolic modulation of the LC birefringence. Both the phase delay and the focal length have been calculated for the different values of V and the lens aberrations have been estimated.

Noteworthy, LC lens with a parabolic phase profile have recently been proposed [7]. In that work the parabolic profile was obtained by a proper electrode pattern that gave rise to a parabolic distribution of the applied voltage. Our approach, on the contrary, is based on photoalignment and does not require any electrode patterning.

Preprints (www.preprints.org) | NOT PEER-REVIEWED | Posted: 27 June 2023 doi:10.20944/preprints202306.1931.v1

1. Modeling the LC lens

Let us consider a nematic liquid crystal (LC) cell of thickness L and width D with spatially modulated anchoring. Specifically, we assume strong planar anchoring at the top substrate, and an anchoring energy dependent on the distance from the center of the cell at the bottom substrate [18]. A sketch of the cell is reported in Figure 1. In this figure the OZ axis passing through the cell center and perpendicular to the plane of the cell is shown together with the lens width D and the lens aperture R.

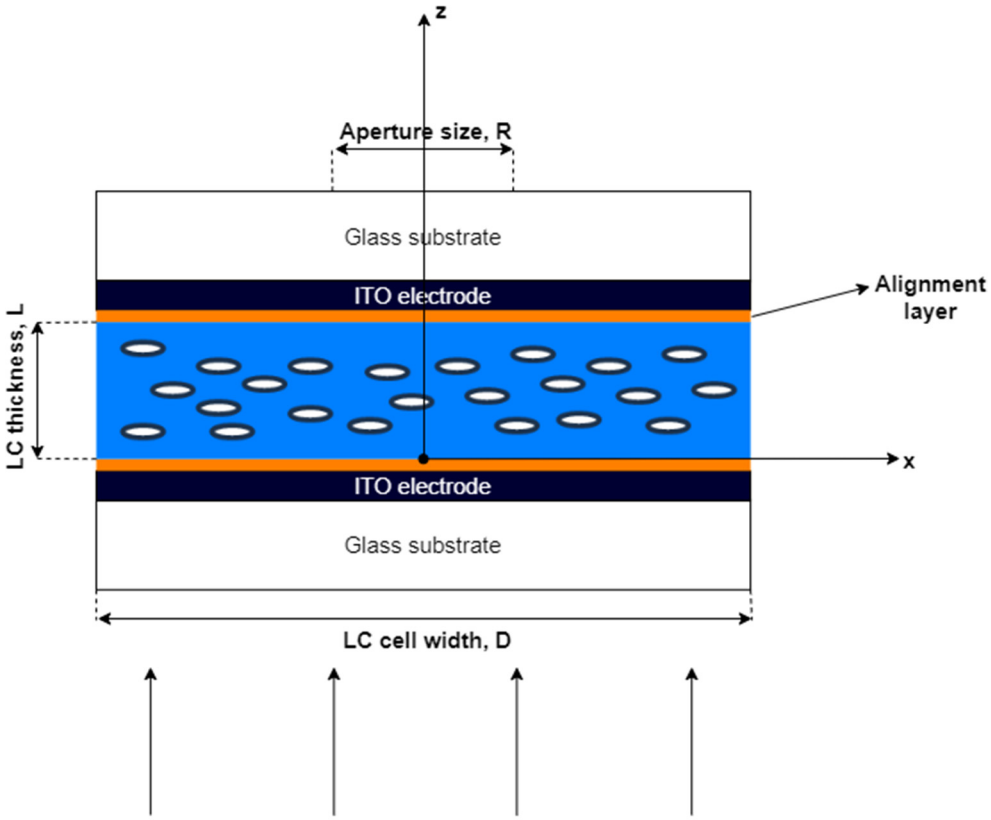

Figure 1. Scheme of the LC cell giving rise to the proposed LC lens. The four vertical arrows represent a test light beam impinging on the cell.

When a proper external voltage V is applied to the cell along Z, the LC director $\boldsymbol{n}$ reorients by an amount that depends both on the value of V and on the value of the anchoring energy $W(x)$. Being the anchoring spatially modulated, this reorientation is modulated as well, thus giving rise to a lens-like refractive index profile. The focal length of the resulting lens depends on the applied voltage and is thus electrically tunable.

We assume an anchoring energy profile $W(x)$ at the bottom substrate of the cell of the form:

$$W(x) = \begin{cases} W_1, & 0 \le x \le (D-R)/2 \\ 2W_1 - \frac{W_1\left(x-\frac{D}{2}\right)^2}{\left(\frac{R}{2}\right)^2}, & (D-R)/2 \le x \le (D+R)/2 \\ W_1, & (D+R)/2 \le x \le D \end{cases} \quad (1)$$

where D is the lens width, R the lens aperture and W_1 the constant minimum anchoring energy (see Table 1). $W(x)$ is shown in Figure 2. The value of W_1 has been chosen based on previous investigation [16,17,19].

Preprints (www.preprints.org) | NOT PEER-REVIEWED | Posted: 27 June 2023 doi:10.20944/preprints202306.1931.v1

Table 1.

1	D	$12x10^3\ \mu m$	lens width
2	R	$6x10^3 \mu m$	aperture of the lens
3	W_1	$10^{-6}\ \frac{J}{m^2}$	Minimum anchoring energy
4	K_{11}	$6 \cdot 10^{-12}\ N$	Splay elastic constant
5	K_{33}	$25 \cdot 10^{-12}\ N$	Bend elastic constant
6	L	$50\ \mu m$	LC cell thickness
7	ω	$10^3 Hz$	AC electric field frequency
8	σ	$10^{-8}\ \frac{S}{m}$	LC electric conductivity
9	$\varepsilon_\perp$	5.1	LC dielectric constant in the direction perpendicular to **n**
10	ε_0	$8.8542 \cdot 10^{-12}\ \frac{F}{m}$	Vacuum dielectric constant
11	$\varepsilon_{\|\|}$	13.7	LC dielectric constant in the direction parallel to **n**
12	θ_2	$\frac{\pi}{180}\ rad$	Direction of easy axis at the up substrate (pretilt angle)
13	V	$(0.7-1)\ V$	Applied voltage to the cell
14	θ_1	$\frac{\pi}{180}\ rad$	Direction of easy axis at the bottom substrate (pretilt angle)

We model a cylindrical lens, which allows simplifying the problem to the 2D case with respect to the 3D approach required for conventional spherical lenses.

2. Director Reorientation under action of externally applied voltage in the cell with modulated anchoring energy

To investigate the electro-optical properties of the proposed LC lens, one needs to find the director reorientation angle $\theta(x,z)$. Noteworthy, we suppose that the LC director reorientation induced by the externally applied voltage occurs in XZ-plane therefore this is the only angle one needs to calculate.

The director field has the form $\boldsymbol{n} = \left(\cos\theta\,(x,z), 0, \sin\theta\,(x,z)\right)$ and the total free energy density F is given by:

$$\mathcal{F} = \mathcal{F}_{elasic} + \mathcal{F}_{electric} + \mathcal{F}_{surface}, \tag{2}$$

where:

$$\mathcal{F}_{elastic} = \int_V \left(\frac{K_{11}}{2}\mathrm{div}(\boldsymbol{n})^2 + \frac{K_{22}}{2}\left(\boldsymbol{n}\cdot\mathrm{curl}(\boldsymbol{n})\right)^2 + \frac{K_{33}}{2}[\boldsymbol{n}\times\mathrm{curl}(\boldsymbol{n})]^2\right) dV, \tag{3}$$

is the elastic free energy density,

$$\mathcal{F}_{electric} = -\frac{1}{2}\int_V (\boldsymbol{D}\cdot\boldsymbol{E})dV, \tag{4}$$

represents the dielectric coupling with the external electric field, and the surface part of the total free energy density reads [20]:

$$\mathcal{F}_{surface} = -\frac{1}{2}\sum_{S_i}\int_{S_i} W_i(\boldsymbol{d}\cdot\boldsymbol{n})^2 dS_i, \tag{5}$$

here K_{ii} are the LC elastic constants, $\boldsymbol{D}$ is the electric displacement vector, $\boldsymbol{E}$ is the externally applied electric field, $\boldsymbol{d}$ is the easy axis direction and W_i (i=1,2) is the anchoring energy at LC cell bounding substrates.

Substituting equations (3)–(5) in eq. (2) and minimizing F, one obtains the following Euler-Lagrange equation for $\theta(x,z)$:

Preprints (www.preprints.org) | NOT PEER-REVIEWED | Posted: 27 June 2023 doi:10.20944/preprints202306.1931.v1

$$\theta_{xx}(K_{11}sin^2\theta + K_{33}cos^2\theta) + \theta_{zz}(K_{11}cos^2\theta + K_{33}sin^2\theta) + (K_{33} - K_{11})[(\theta_z^2 - \theta_x^2)\sin\theta\cos\theta + \theta_{xz}\sin 2\theta + \theta_x\theta_z\cos 2\theta] + \varepsilon_0\varepsilon_\alpha(\sin\theta\cos\theta(E_z^2 - E_x^2) + E_zE_x\cos 2\theta) = 0 \quad (6)$$

where $\varepsilon_a = \varepsilon_{||} - \varepsilon_\perp$ is the LC dielectric anisotropy, i.e. the difference between the dielectric constants in the directions parallel and perpendicular to **n**.

Considering finite director anchoring at the bottom substrate and strong anchoring at the top substrate, the boundary conditions take the form:

$$\begin{cases} [(K_{33}sin^2\theta + K_{11}cos^2\theta)\theta_z]|_{z=0} - W(x)\sin(\theta(0) - \theta_1)\cos\theta(0) - \theta_1 = 0, \\ \theta(z = L) = \theta_2 \end{cases} \quad (7)$$

Equations (6) and (7) should be accompanied by the Poisson equation for the electric field potential U, defined by the relation $\boldsymbol{E} = -\boldsymbol{\nabla}U$ [18]

$$\boldsymbol{\nabla}\left(\tilde{\varepsilon}\varepsilon_0\boldsymbol{\nabla}\,U(x,z)\right) = 0, \quad (8)$$

where $\tilde{\varepsilon}\varepsilon_0 = \hat{\varepsilon}\varepsilon_0 + i\frac{\sigma}{\omega}$, being $\tilde{\varepsilon}$ the permittivity tensor, ω the AC electric field frequency, σ the LC electric conductivity and $\hat{\varepsilon}$ the LC dielectric tensor. In our case this latter has the form:

$$\hat{\varepsilon} = \begin{pmatrix} \varepsilon_\perp + \varepsilon_a\cos^2\theta & 0 & \varepsilon_a\sin\theta\cos\theta \\ 0 & \varepsilon_\perp & 0 \\ \varepsilon_a\sin\theta\cos\theta & 0 & \varepsilon_\perp + \varepsilon_a\sin^2\theta \end{pmatrix}, \quad (9)$$

The electric field potential $\mathrm{U}(x,z)$ obeys the following boundary conditions:

$$\begin{cases} \mathrm{U}|_{z=0} = 0 \\ \mathrm{U}|_{z=L} = V' \end{cases} \quad (10)$$

where V is voltage applied to the cell at $z = L$.

In this way, one gets the following system of equations for the director field $\theta(x,z)$ and for the electric field potential $\mathrm{U}(x,z)$ with boundary conditions:

$$\begin{aligned} &\theta_{xx}(K_{11}sin^2\theta + K_{33}cos^2\theta) + \theta_{zz}(K_{11}cos^2\theta + K_{33}sin^2\theta) \\ &\quad + (K_{33} - K_{11})[(\theta_z^2 - \theta_x^2)\sin\theta\cos\theta + \theta_{xz}\sin 2\theta + \theta_x\theta_z\cos 2\theta] \\ &\quad + \varepsilon_0\varepsilon_\alpha(\sin\theta\cos\theta(E_z^2 - E_x^2) + E_zE_x\cos 2\theta) = 0 \\ &\boldsymbol{\nabla}\left(\tilde{\varepsilon}\varepsilon_0\boldsymbol{\nabla}\,U(x,z)\right) = 0 \\ &[(K_{33}sin^2\theta + K_{11}cos^2\theta)\theta_z]|_{z=0} - W(x)\sin(\theta(0) - \theta_1)\cos(\theta(0) - \theta_1) = 0 \\ &\quad \theta(z = L) = \theta_2 \\ &\mathrm{U}|_{z=0} = 0 \\ &\mathrm{U}|_{z=L} = V \end{aligned} \quad (11)$$

The system of equations (11) has no analytical solution. To solve it, it is necessary to use computer calculations. The parameters we used for calculations are reported in Table 1. The values selected for the splay, K_{11}, and bend, K_{33} elastic constants are of the order of those typical of the most common thermotropic LCs [18, 21].

The electric field potentials calculated for $V = 1\,V$ and $V = 0.8\,V$ at the middle of the cell z = L/2, as a function of x, are reported in Figure 3a and 3b, respectively. Figure 4 shows the LC director profile vs x for the same values of V at z = L/2. As expected, it follows the profile of the electric field potential.

Preprints (www.preprints.org) | NOT PEER-REVIEWED | Posted: 27 June 2023 doi:10.20944/preprints202306.1931.v1

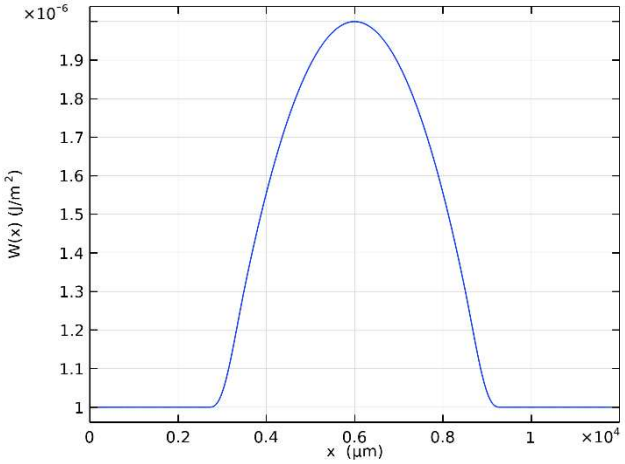

Figure 2. Spatial profile of anchoring energy $W(x)$ at the bottom substrate.

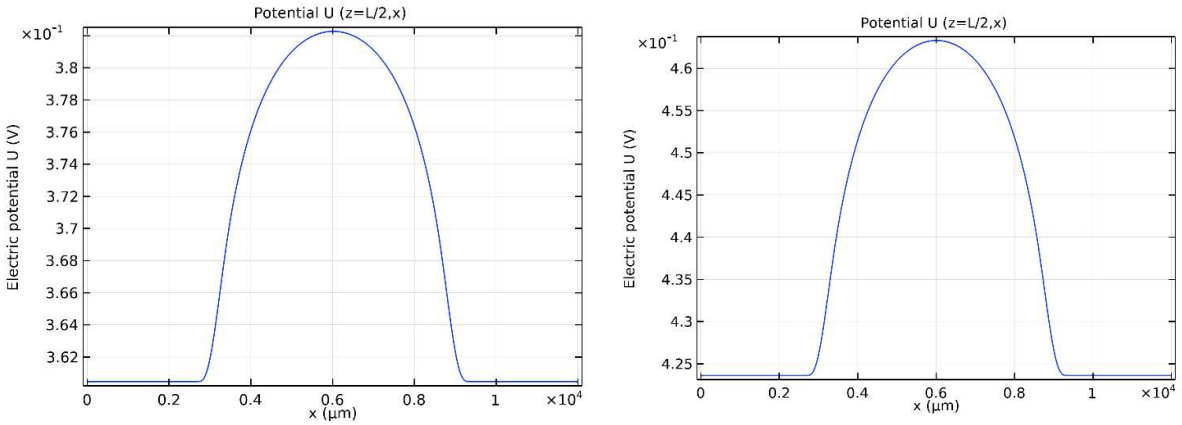

Figure 3. Electric potential U versus x at z = L/2 for V = 0.8 V (a) and V = 1 V (b).

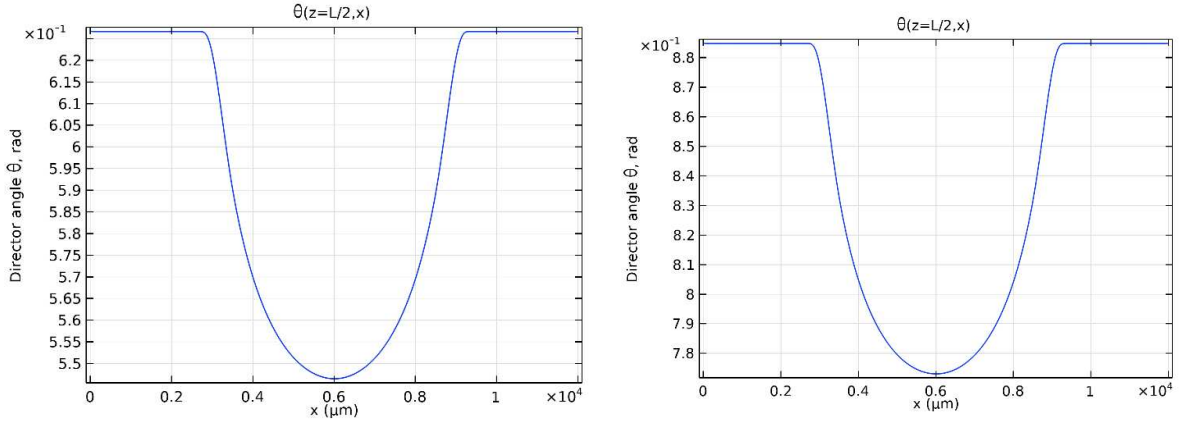

Figure 4. LC director profile at z = L/2 as a function of the distance x from the center of the cell for V = 0.8 V (a) and v = 1 V (b).

3. Light propagation through LC cell subject to externally applied voltage

In the previous section, we have calculated the spatial profile of the LC director subject to an externally applied voltage. The refractive index for an extraordinary beam propagating in the LC cell is given by the relation:

Preprints (www.preprints.org) | NOT PEER-REVIEWED | Posted: 27 June 2023 doi:10.20944/preprints202306.1931.v1

$$n_{eff}(\psi) = \frac{n_0 n_e}{\sqrt{n_e^2 \cdot \cos^2(\psi) + n_0^2 \cdot \sin^2(\psi)}}, \quad (12)$$

where ψ is the angle between the LC director (which defines the optical axis) and the light wave vector. In our case $\psi = \frac{\pi}{2} - \theta$.

We treat the LC cell with a lens-like director distribution as a thin phase plate. The phase retardation ϕ experienced by a test light beam propagating through the cell is defined as

$$\phi = \frac{2\pi}{\lambda} \int_0^L n_{eff}(\theta)\, dz \quad (13)$$

and depends on the distance x from the center of the cell. This is shown in Figure 5 for different values of the applied voltage V. This dependence determines the focusing properties of the LC lens.

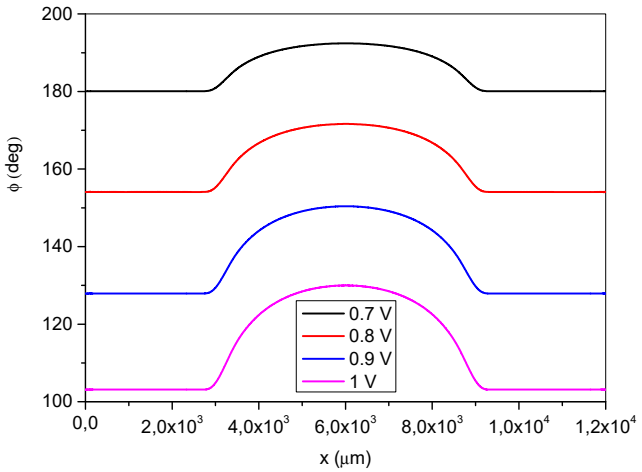

Figure 5. Dependence of the phase retardation $\phi(x)$ on the distance x for different values of the applied voltage *V*.

To evaluate the focal length of the LC lens, we fit the curves $\phi = \phi(x)$ in Figure 5 to a parabola according to the paraxial approximation [22,23] using the equation:

$$\phi(x) = a - \frac{kx^2}{2f}, \quad (14)$$

being $a = \phi(0)$ the phase shift at the center of the LC cell, f the focal length of the LC lens and k the modulus of the test beam wave vector.

The inverse of the obtained focal length is shown in Figure 6 as a function of the applied voltage *V* for a lens aperture R = 1mm. The electrical tunability of the lens focus is well represented by this curve.

Preprints (www.preprints.org) | NOT PEER-REVIEWED | Posted: 27 June 2023 doi:10.20944/preprints202306.1931.v1

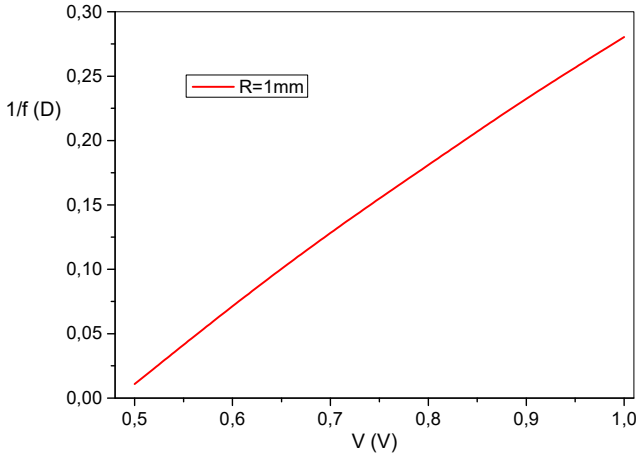

Figure 6. Dependence of LC lens power on applied voltage. Lens aperture R = 1mm.

4. Aberration of LC Lens with modulated anchoring energy

Optical lenses, and LC lenses do not make exception, are not ideal optical systems. Indeed, there is always some degree of aberration introduced by the lens, which causes the image to be an imperfect replica of the object. Aberration thus plays an important role in the formation of images and among them spherical aberration is the most common when dealing with monochromatic light.

Figure 7 shows the definition of spherical aberration. A spherically aberrated lens has no well-defined focus. The distance along the optical axis between the intercept of the rays that are nearly on the optical axis (paraxial rays) and the rays that go through the edge of the lens (marginal rays) is called longitudinal spherical aberration (LSA) [24].

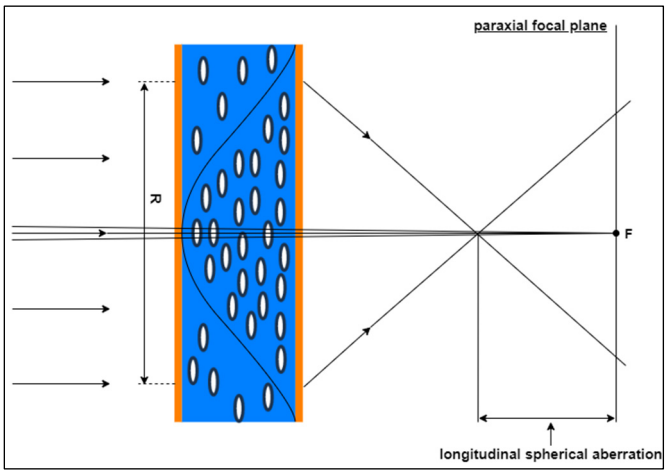

Figure 7. Illustration of the spherical aberration.

Theoretically, to obtain the LSA in a LC lens it is necessary to find the beam trajectory in an inhomogeneous liquid crystal cell [25,26]. Here we propose a simpler and quicker approach.

In the previous section, to find the focal length of the LC lens we used the paraxial approximation, that holds for a beam that is as close as possible to the optical axis of the lens [22], as well as for an ideal spherical wavefront. However, as the aperture of the lens R increases, this approximation is less and less fulfilled.

Preprints (www.preprints.org) | NOT PEER-REVIEWED | Posted: 27 June 2023 doi:10.20944/preprints202306.1931.v1

In Figure 8 one can see the phase retardation (eq. 13) compared to the one modeled using the paraxial approximation (eq. 14) for different lens apertures R = 1 mm (a) and R = 3 mm (b), for an applied voltage V = 0.7 V. As R increases from 1 to 3 mm, the quality of the approximation worsens, which indicates that we have an imperfect lens and aberrations must be estimated.

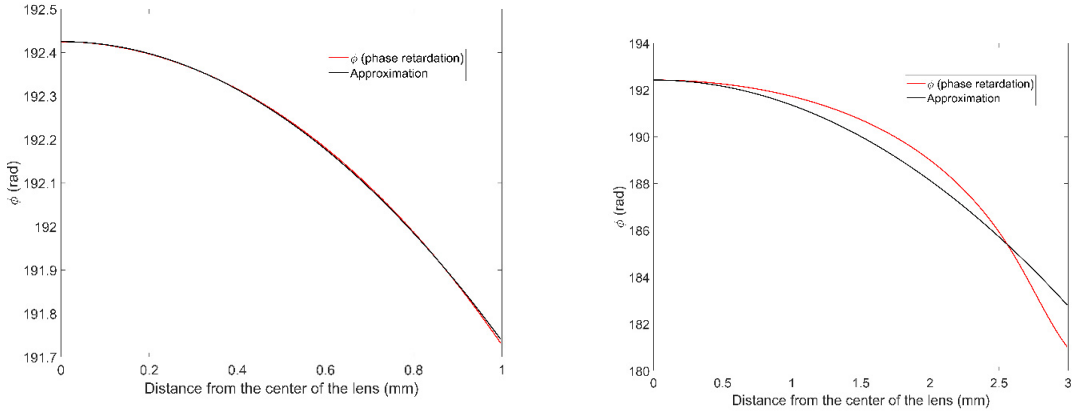

Figure 8. Comparison between the phase retardation given by eq (13) and the one modeled by eq. (14) for different values of the lens aperture: R=1 mm (a) and R=3 mm (b).

To estimate the LSA, we found where the beam come from the edge of the lens aperture. To this aim we used the paraxial approximation (14) to describe the beam wavefront near the lens aperture point. Mathematically, this means that we have approximated a part of the wavefront near the lens aperture and found the approximation coefficients. Next, we found a point on the axis of this parabola, where the rays from the edge of the aperture converge. Using mathematical formulas, we projected it onto the axis of the lens. Thus, we got the point where the rays will come from the edge of the lens (lens aperture).

Figure 9 shows the relative longitudinal spherical aberration, defined as the ratio between the LSA and the focal length, versus the lens aperture R, for V = 0.8 V (black line) and V = 1 V (red line).

The relative longitudinal spherical aberration as a function of the applied voltage at fixed values of R (R = 1.5 mm and R = 2 mm) is instead reported in Figure 10 a and b.

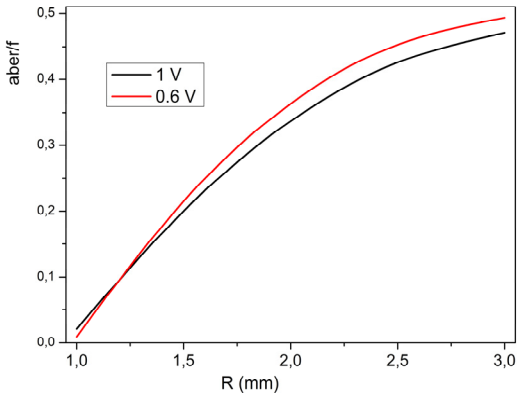

Figure 9. Relative longitudinal aberration as a function of the lens aperture R, for V = 0.6 V (red line) and V = 1 V (black line).

Preprints (www.preprints.org) | NOT PEER-REVIEWED | Posted: 27 June 2023 doi:10.20944/preprints202306.1931.v1

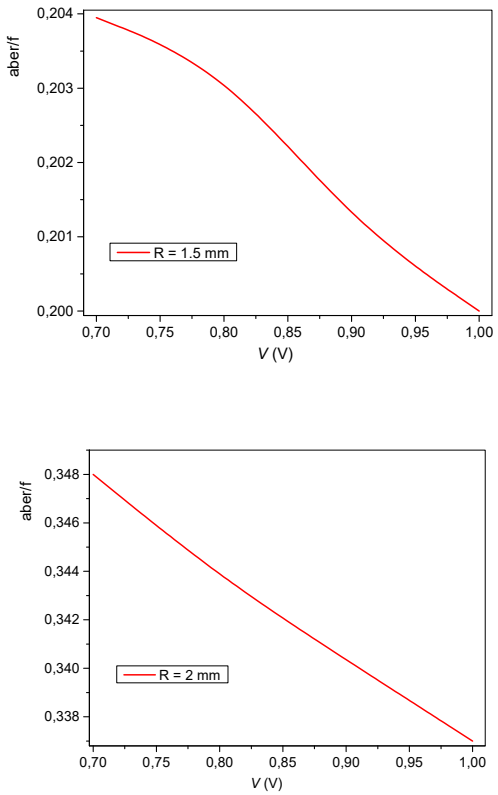

Figure 10. Relative longitudinal aberration as a function of the applied voltage V, for R = 1.5 mm (a) and R = 2 mm (b).

The relative LSA increases with R, as expected, and slightly decreases with increasing V, which we understand as a voltage-induced change in the phase profile. The increasing voltage makes the phase profile "more parabolic".

5. Conclusion

We proposed a theoretical model that describes the properties of a cylindrical LC lens with parabolic phase profile induced by a spatially modulated anchoring energy. We have calculated the director profile, the electric field potential in the LC cell and the phase delay experienced by a light beam propagating through the cell. Moreover, we have estimated the focal length and the longitudinal spherical aberration of the LC lens. The dependence of the focal length on the applied voltage demonstrates the electrical tunability of the modeled lens.

The observed dependence of the lens aberration on the external voltage and on the lens aperture allows optimizing the lens features to get the best image quality. As an example, combining f and LSA, it is possible to look for the conditions giving the highest optical power with the lowest aberrations. The obtained results can easily be applied to experimentally developed LC lenses. Indeed, in principle photoalignment allows to obtain different profiles of the anchoring energy so that the phase retardation can become closer to the parabolic profile in a wide range of externally applied voltages, thus reducing the aberrations. We expect that AI or machine learning can also help to find the optimal profile of the anchoring energy.

Proper experiments will be soon under way to validate the above predictions.

References

1. S. Sato, Jpn. J. Appl. Phys. 18, 1679 (1979).
2. N.A. Riza and M.C. DeJule, Opt. Lett. 19, 1013 (1994).
3. H. Ren and S.T. Wu, Appl. Phys. Lett. 82, 22 (2003).

4. M. Ye, Y. Yokoyama and S. Sato, Appl. Phys. Lett. 89, 141112 (2006).
5. M. Ye, B. Wang and S. Sato, Opt. Commun. 259, 710 (2006).
6. J. F. Algorri, P. Morawiak, N. Bennis, D. C. Zografopoulos, V. Urruchi, L. Rodríguez- Cobo, L. R. Jaroszewicz, J. M. Sánchez-Pena, J. M. López-Higuera, Sci. Rep. 10:10153 (2020).
7. W. Feng, Z. Liu, H. Liu and M. Ye, Crystals 13, 8 (2023).
8. L. Lucchetti, J. Tasseva, Appl. Phys. Lett. 100, 181111 (2012).
9. J. F. Algorri, D. C. Zografopoulos, V. Urruchi, J. M. Sánchez-Pena, Crystals, 9, 272 (2019).
10. T. Zhan, Y.-H. Lee, G. Tan, J. Xiong, K. Yin, F. Gou, J. Zou, N. Zhang, D. Zhao, J. Yang, S. Liu, S.-T. Wu, J. Opt. Soc. Am. B 36, D52 (2019).
11. Y. Ma, A. M. W. Tam, X. T. Gan, L. Y. Shi, A. K. Srivastava, V. G. Chigrinov, H. S. Kwok, J. L. Zhao, Opt. Exp. 27, 10079 (2019).
12. A. Jamali, D. Bryant, Y. Zhang, A. Grunnet-Jepsen, A. Bhowmik, P. J. Bos, Appl. Opt. 57, B10 (2018).
13. H.-Y. Lin, N. Avci, S.-J. Hwang, Liq. Cryst. https://doi.org/10.1080/02678292.2018.1562114 (2019).
14. A.G. Dyadyusha, T. Ya. Marusii, Yu. A. Reznikov, A.I. Khizhniak, V. Yu. Reshetnyak, JETP Letts, 56, 17-21 (1992).
15. M. Schadt, H. Seiberle, A. Schuster, Nature, 381, 212–215 (1996).
16. V.G. Chigrinov, V.M. Kozenkov, H. Kwok, Photoalignment of liquid crystalline materials: physics and application, John Wiley&Sons, Ltd, Publication, 231 (2008).
17. D. Alexei, V. Kiselev, V.G. Chigrinov, D.D. Huang, Phys. Rev. E 72, 061703 2005, 2005.
18. V. Yu. Reshetnyak, O. Sova, Yu-Jen Wang, Yi-Hsin Lin, Proc. SPIE 11303, Emerging Liquid Crystal Technologies XV, 1130304 (2020).
19. K. Takatoh, M. Hasegawa, M. Koden, N. Itoh, R. Hasegawa and M. Sakamoto, Alignment Technologies and Applications of Liquid Crystal Devices, Taylor & Francis Oxon OX14 4RN, ISBN 0-748-40902-5 (2005).
20. P. G. de Gennes and J. Prost, The Physics of Liquid Crystals, 2nd edition, Clarendon Press, Oxford, 1993, 614 p.
21. L. Lucchetti, G. Nava, R. Barboza, F. Ciciulla, T. Bellini, J. Mol. Liq., 329, 115520 (2021)
22. J.W. Goodman, Introduction to Fourier Optics (McGrawHill, New York, 2002).
23. Yi-Hsin Lin, Yu-Jen Wang and V. Yu. Reshetnyak, Liquid Crystals Reviews, 5, 111, (2017).
24. M. Born and E.W. Wolf, Principles of Optics (Pergamon Press, Oxford, 1991).
25. S. Valyukh, V.G. Chigrinov, H.S. Kwok, SID 08 DIGEST, pp 659-662 (2008).
26. S. Bielykh, S. Subota, V. Reshetnyak, T. Galstian, Ukr. J. Phys., 55, 294 (2010).
27. J.W. Goodman, Introduction to Fourier Optics, McGraw Hill, New York (2002)